International Journal of Applied Engineering Research ISSN 0973-4562 Volume 13, Number 3 (2018) pp. 1567-1577

Fire Hazard Map by Combining Landsat Data Classification and Topography Map of Pekan Study Area

[1]Mohamad Eliyass Bin Jamaruppin, [1,3*]Luhur Bayuaji, [1]Ngahzaifa Ab Ghani, [4]Farid Wajdi Akashah, [4]Azlan Shah Ali, [2,3]Dwi Pebrianti and [3]Indra Riyanto

[1] Faculty of Computer Systems & Software Engineering, Universiti Malaysia Pahang, Malaysia.
[2] Faculty of Electrical & Electronics Engineering, Universiti Malaysia Pahang, Malaysia.
[3] Magister Ilmu Komputer, Universitas Budi Luhur, Indonesia.
[4] Faculty of Built Environment, Universiti Malaya, Malaysia.
[*] Corresponding Author

Abstract

Forest fire, that occurs annually in peat land area around Jalan Kuantan-Pekan, Pahang, Malaysia, is endangering the surrounding area. It is become important to create the fire hazard map in order to minimize the potential damage. The data survey, as conventional method to create the fire hazard map, has a drawback such as time and cost consuming. Remote sensing and geographic information system (GIS) have been used in this study as alternative method to derive the map by exploiting the information from Landsat 8 image and topographic map at study area. Landsat 8 was exploited to extract the fuel type by using maximum likelihood supervise classification. The buffer zone area will be created from topographic map. By combining of the fuel type data and buffer zone area, the hazard area can be estimated by using spatial analysis method. The result shows that most of the study area is in low and moderate hazard level. While final result shows only 5% of areas of high and extreme but it is quite dangerous to the residents and school community around the study area that covers more than 10,000 lives.

Keywords: Remote sensing; GIS; fire hazard; MLC; topographic map

INTRODUCTION

Forest fire is a worldwide issue in many biodiversity that was influenced by global warming and other causes [1-5]. Generally, the high temperature condition or El Nino in the natural forests increase the rate of fire hazard into large scale forest fire [6].

Globally, forest fire responsible for burning more than 350 million hectares of forest land every year [7]. There are about 2 to 8 million acres was burn annually from mid-1980 through 2015 in United States [8, 9]. In Malaysia, 1,232 fires have been reported from 1992 to 1998 and about 5.55 million hectares or 42.2% of Malaysia peninsular forest land area [10]. In average, more than 2000 forest and bush was record every month in the year 2014 – 2016 was recorded by Malaysia Fire and Rescue Department (JBPM) [11]. The area in this study is also no exception to face forest fire problem annually [12-15]. In general, forest fire is perceived as a threat that causes economic losses, animal habitat destruction, health hazard, etc. Indeed, forest fire prediction and prevention are become crucial. How to create forest fire hazard map that is suitable to Malaysian forest characteristics becomes the biggest question to be solved.

Since the mid-1980s, remote sensing and geographic information system (GIS) has been implement as a technique to estimate forest fire occurrence and fire hazards [16]. Several studies also have been done in developing the forest fire risk mapping using this technique [9, 17-22]. Remote sensing technique will retrieve several information from satellite image, then integrate with topographic map in GIS format. Several satellite image data can be processed by using remote sensing technique such as Moderate Resolution Image Spectro radiometer (MODIS) image [18, 20, 23, 24], ASTER image [25-27] and Sentinel 2 satellite image [28-31].

On preparing the forest fire hazard map, study area data collection is important step. Generally, data was collected by conducting in-situ data collection. However, it will cost time and money [32, 33]. In this study, several important data will be derived using remote sensing technique applied on satellite images whilst other data will be collected from various sources. Remote sensing as alternative method of data collection will not only reduce cost and time, but also get data in both spatial and temporal domains. In order to developed the forest fire hazard map, spatial analysis technique will be applied.

Objective of this study is to create fire hazard map by utilizing remote sensing and geographic information systems (GIS). In this study, Landsat 8 and topographic map will be used to analyse the forest fire in study area. The study area located in Pahang state of Malaysia and faced forest fire problem annually [11, 12, 15, 34-38]. According to the author's knowledge, this paper is the first study using Landsat 8 for forest fire in peat land to this study area.

STUDY AREA

The study area is located at Jalan Kuantan-Pekan, Penor Pahang, Malaysia with longitude between 103°14 to 103°17 East and latitude between 3°42 to 3°45 North as shown in Figure 1. This area covered approximately 2,480.95 ha. Newly established residential area and palm oil plantation are bordering the study area. Annually, the study area peat swamp forests were destroyed by fire. The study area is equatorial, the climate is the low seasonal variation in incoming solar radiation [39]. The annual average temperature ranges from 20.5° Celsius (C) to 36° C [40].

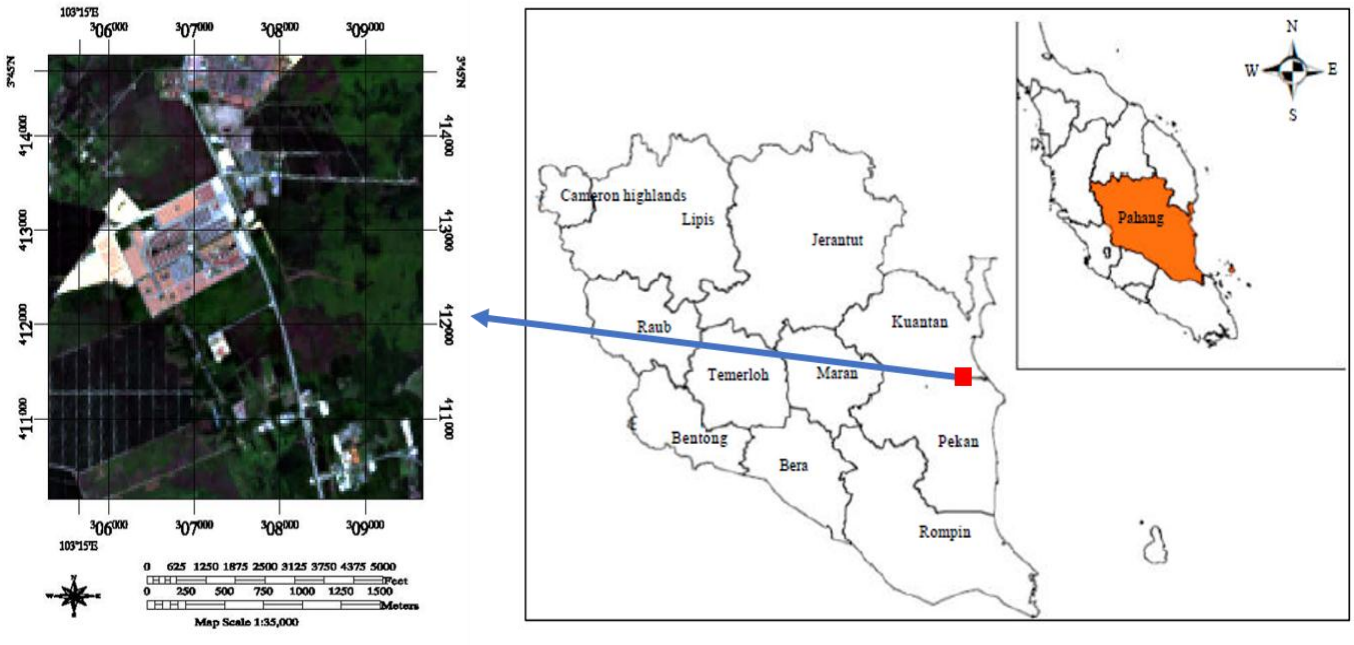

Figure 1. Study Area in Pekan, Pahang.

DATA AND METHOD

A. Data

Satellite image and topographic map of study area will be utilized to create fire hazard map. A Landsat 8 image data of study area, acquired on 26 June 2016, will be used. The Landsat data located at path 126 and row 57. This Landsat image was an excellent source because acquire under cloud-free conditions in order to extract various types of fuel in the study area. Clouds and their shadows will distract the result by provide inaccurate reflectance values of the features in the Landsat image earth surface and disrupt the classification. Therefore, the image that covered by clouds is not include in this study [41]. The overall data processing method for this study are shown in Figure 2. Image pre-processing for this study mainly include atmospheric correction using Fast Line-of-sight Atmospheric Analysis of Hypercubes (FLAASH), subset, Maximum Likelihood Classification (MLC), Confusion matrix for accuracy assessment and fuel type mapping. In this case, several information will be retrieved from topography map, such as road, residence and buffering zone. Forest fire hazard map will be derived by integrating the information from Landsat image and topographic map.

B. Image pre-processing

Atmospheric correction is land surface assumption on quantitative analysis parameter via remote sensing data. Atmospheric correction is to decrease or remove atmosphere effect such as molecule and aerosol on the reflectance values [41]. Fast Line-of-sight Atmospheric Analysis of Hypercubes or FLAASH is the fundamental concept for atmospheric correction tool in most hyperspectral and multispectral sensors that improve wavelengths up to 3 µm for visible through near-infrared and shortwave infrared regions [42]. Vertical (nadir) or slant-viewing geometries image also can correct by FLAASH [43]. FLAASH also can correct the adjacency effect, compute a scene-average visibility, and adjustable spectral polishing for artifact suppression [44]. The standard equation for spectral radiance at a sensor pixel, L, id the initial of FLAASH before solar wavelength range (neglect the thermal emission) and flat, Lambertian materials or their equivalents. The equation is as follows:

$$L = \left(\frac{A\rho}{1-\rho_e S}\right) + \left(\frac{B\rho_e}{1-\rho_e S}\right) + L_a \quad , \qquad (1)$$

where;

ρ is the pixel surface reflectance,

ρ_e is an average surface reflectance for the pixel and a surrounding region,

S is the spherical albedo of the atmosphere,

L_a is the radiance back scattered by the atmosphere,

A and B are coefficients that depend on atmospheric and geometric conditions but not on the surface.

All these attributes rely on the spectral channel and for simplicity the wavelength index has been exclude. Radiance that is reflected from the surface and send directly to sensor is the first term, while radiance from the surface that is scattered by the atmosphere into the sensor is the second term in the equation. Pixel surface reflectance in all the sensor channels solved after the water retrieval is performed.

Remote sensing commonly used calibration imagery as pre-processing to create scientific products from images [45]. In order to produce an image that represents true spectral radiance at the sensor, radiometric errors from sensor defects, variations in scan angle, and system noise will be compensate in calibration attempts [46]. Calibrated digital numbers before output to the distribution media represented by eight-bit value scaled to give absolute radiance [47].

Subset is to crop Landsat data for the study area. The main purpose of this method is for focusing to the study area only. If include all areas that unrelated to the studies may cause inaccurate result. Subset Data from ROIs to subset data into a rectangle that contains the selected ROIs of study area [48, 49].

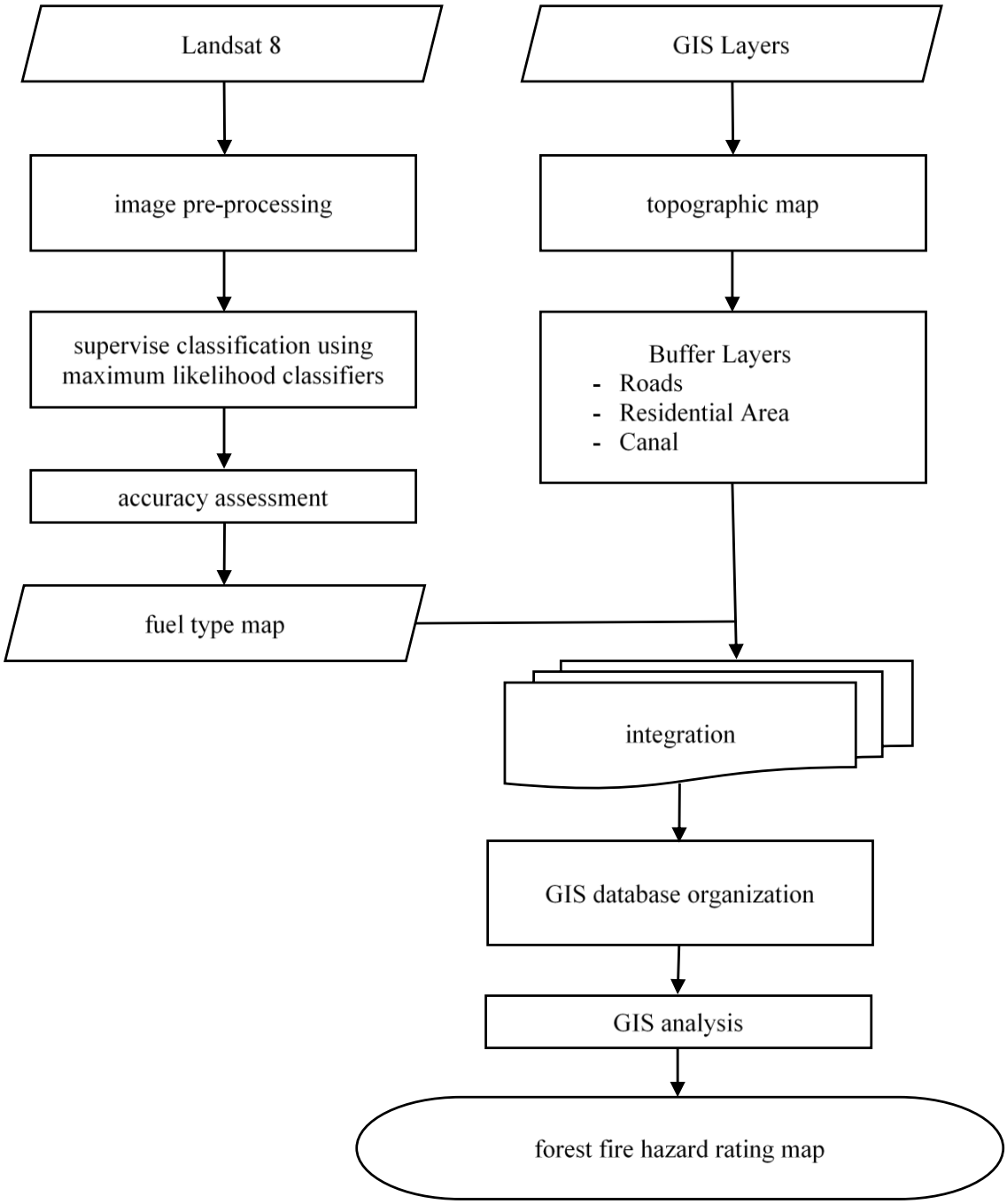

Figure 2. Process flow hazard map by combining Landsat data classification and GIS topography map

C. Land cover classification method

MLC is a supervised classification method which is based on the Bayes theorem. The MLC representing classes into the signature file by combining both variances and covariances of the class signatures. Pixel will assigned by discriminant function to get highest likelihood class [50]. Class mean vector and covariance matrix are the key inputs to the function and can be estimated from the training pixels of a particular class[51]. In this study, we used MLC to classify a diverse tropical land covers recorded from Landsat 8 satellite. The classification is carefully examined using visual analysis, classification accuracy, band correlation and decision boundary. The formula of MLC that are using in this study are shown below.

$$g_i = 1n\, p(\omega_i) - {}^1/_2\ 1n\,|\Sigma_i| - {}^1/_2\,(x-m_i)^{\tau}\Sigma_i^{-1}(x-m_i), \quad (2)$$

where;

i = class,

x = n-dimensional data (where n is the number of bands),

p(ωi) = probability that class ωi occurs in the image and is assumed the same for all classes,

|Σi| = determinant of the covariance matrix of the data in class ωi,

Σi-1 = its inverse matrix,

mi = mean vector.

In MLC, each class in study area are in multispectral space where larger classes is a discriminant function to other classes [52]. The general procedures in MLC are to determine the number of land cover types, every desired classes collected the training pixels via land cover information, then each class mean vector and covariance matrix were estimated by training pixels, and finally land cover types were classified from every pixel in the image [53].

Accuracy assessment in MLC were define by confusion matrix or error matrix means. It compares the relationship between ground truth reference data and the corresponding results of a classification on a class-by class basis [54]. The number of classes is equal to square matrices include the number of rows and columns. Producer accuracy is a accuracy measurement for particular classification scheme by showing the total of correct classified on particular ground class in percentage [52]. It is calculated by dividing total of each elements in ground truth pixel and MLC pixel diagonally:

$$\text{Producer accuracy} = \frac{c_{aa}}{c_{*a}} \times\ 100\%, \quad (3)$$

where,
c_{aa} = element at position a^{th} row and a^{th} column,

c_{*a} = column sums

User Accuracy is used to measure of the performance classification. It indicates the percentage of probability that the class which a pixel is classified to on an image represents that class on the ground. It is calculated by dividing each of the diagonal elements in a confusion matrix by the total of the row in which it occurs:

$$\text{User accuracy} = \frac{c_{ii}}{c_{*i}} \times\ 100\%, \quad (4)$$

where,
c_{ii} = value of class, c_{*i} = row sum.

A measure of overall behavior of the MLC can be determined by the overall accuracy, which is the total percentage of pixels correctly classified where the total number of pixels and classes respectively.

D. Topographic map & fire hazard rating index (FHRI) modelling

Topographic map is two-dimensional representation of a portion of the three-dimensional surface of the earth. Topography exist to represent the land surface by shaping of the land surface [55]. In this research, topographic map is a detailed and accurate the illustration of man-made and natural features on the ground such as roads, canal, resident area, school, water area, clear land, oil palm plantation and geographic names.

Topographic map will build buffer layer for road, canal, and resident area. The buffer is classes base on the gap of human access to the prediction of fire locator. On the other hand, the fuel type classes will be classified based on fire hazard rating index in Table 1, for example, null index will include water and canal area, low index will include bare land and road area, etc.

Fire hazard ratings index play as indication for the consequences of fire, if fire was to start. The dangerous conditions were determined by level of fire danger scale, the higher fire danger will cause more dangerous the conditions. Null level is considered as the area is hard to make or spread fire. Low level fire hazard index may easily start and quickly spread the fire but with minimal involvement of larger or deeper fuels layers. Moderate level increased the risk on surface fires starts. High level may easily start the fire, burn vigorously, and will challenge fire suppression efforts. Extreme level is extremely serious and easily start new fires, spread rapidly, and fire suppression efforts will more challenging. The higher value of FHRI result the higher risk of fire hazard on the study area. This study will retrieve value of FHRI from topographic map that have been process.

RESULTS & DISCUSSION

The outcome of MLC classification after assigning the classes with suitable colours, is shown in Figure 3. Result of the area distribution are 24.1 percent of peat land area, 24.1 percent of bushes area, 19.7 percent of resident area, 11.5 percent of road

area, 7.0 percent of oil palm plantation area, 6.5 percent of burn area, 4.4 percent of canal area, 2.5 percent of bare land area, and less than 1 percent is water area. Luckily, there are no clouds and their shadows are covered on this study area.

Peat land and bushes area covers most of the study area in the scene nearly half of the study area. It is no wonder study area faced forest fire annually as mention in introduction, because the fuel type is highly flammable materials [56]. Most of the resident area and oil palm dominate the northern and south-west parts respectively and surrounded by peat land and bushes area. The condition of resident and oil palm area will cause threat if there are fire hazard occur at the peat land or bushes area. A quite large area of bare land can be seen in the west near to the resident area due to development at that moment, while burn area can be seen mostly in the north-west, north-east and south-east of the image and this area previously was peat land or bushes area. The canal cover around the oil palm area and water area is on Indera Sempurna resident area.

Table 2 shows that all classes possess producer accuracy higher than 75% and it is considered good result base on previous study by other researchers [52, 57]. The highest producer accuracy result was bare land gives 100% and the lowest gives 76.35% from canal area. The relatively reasons of low accuracy from canal area mainly cause by the pixels classified as road by 4% and residential area by 1%. The pixels of oil palm was misclassification due to canal and peat land that share some pixels. Although both canal and road have quite similar physical structure or tend to have similar spectral behaviour and therefore can easily be misclassified as each other but the result show otherwise due to the different wavelength position capture by remote sensing. The minimum acceptable overall accuracy is 85% [58, 59] but in this study MLC yielded an overall accuracy of 97.4% and kappa coefficient 0.97, indicating very high agreement with the ground truth.

Table 1. Fire hazard rating index for modelling

No.	Fuel type layer (F)	Fire Hazard Rating Classification	Fire Hazard Rating Index (FHRI)
1.	Burn Area	High	4
2.	Bushes	High	4
3.	Water	Null	1
4.	Road	Low	2
5.	Canal	Null	1
6.	Peat land	Extreme	5
7.	Resident area	Moderate	3
8.	Bare land	Low	2
9.	Oil palm/plantation	Moderate	3
	Road buffer Layer		**FHRI**
10.	0 – 50 m	Extreme	5
11.	50 – 100 m	High	4
12.	100 – 150 m	Moderate	3
13.	150 – 200 m	Low	2
14.	> 200 m	Null	1
	Canal buffer layer		**FHRI**
15.	0 – 50 m	Extreme	5
16.	50 – 100 m	High	4
17.	100 – 150 m	Moderate	3
18.	150 – 200 m	Low	2
19.	> 200 m	Null	1
	Resident buffer layer		**FHRI**
20.	0 – 50 m	Extreme	5
21.	50 – 100 m	High	4
22.	100 – 150 m	Moderate	3
23.	150 – 200 m	Low	2
24.	> 200 m	Null	1

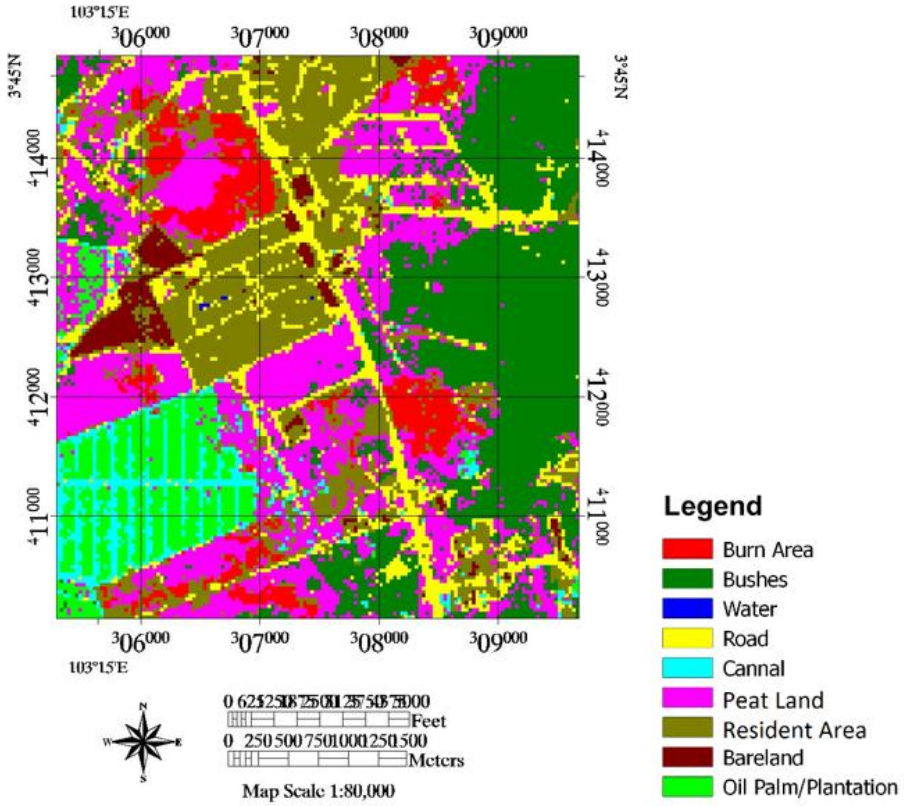

Figure 3. Land cover classification using Maximum likelihood classification

Table 2. Confusion Matrix for MLC

Mapped Class	Ground Truth (Percent)										User Accuracy (%)
	Burn Area	*Water*	*Road*	*Bushes*	*Peat Land*	*Canal*	*Bare land*	*Oil palm*	*Resident Area*	*Total*	
Burn Area	89.47	0.00	0.00	0.00	62.50	0.00	0.00	0.00	0.00	5.79	51.52
Water	0.00	87.50	0.00	0.00	32.65	0.00	0.00	0.00	0.00	1.23	100.00
Road	0.00	0.00	88.31	0.00	0.00	4.08	0.00	0.00	0.00	12.63	100.00
Bushes	0.00	0.00	0.00	100.0	0.00	0.00	0.00	0.00	0.00	19.82	94.44
Peat land	0.00	0.00	0.00	0.00	67.35	0.00	0.00	0.92	0.00	6.14	93.00
Canal	0.00	0.00	0.00	0.00	0.00	94.90	0.00	6.42	0.00	17.54	94.29
Bare land	0.00	0.00	0.00	0.00	0.00	0.00	100	0.00	0.00	4.39	96.00
Oil palm/ Plantation	0.00	0.00	0.00	0.00	0.00	0.00	0.00	92.66	0.00	17.72	85.71
Resident Area	5.26	12.5	11.69	0.00	0.00	1.02	0.00	0.00	98.63	14.74	100.00
Total	100	100	100	100	100	100	100	100	100	100	
Producer Accuracy (%)	89.47	100	87.50	88.31	94.90	76.35	100.0	98.63	92.66		

Result of the fire hazard rating index by transform the maximum likelihood classification image has been shown in Figure 4(a). Every fuel type has been converted into fire hazard rating index value such as water and canal as null risk, road and bare land as low risk, resident area and oil palm/plantation as moderate risk, burn area and bushes as high risk, and peat land as extreme risk. This result was generated by Landsat 8 image processing and classify with FHRI base on level of potential hazard and considered as one of the hazard-index map layer band.

Topographic map such as road map, canal map, and residential map was generated by topology map using QGIS software. In order to calculate the FHRI, the buffer layer has been added to topographic map as details in fire hazard rating index for modelling in table 1. The result after buffer layer was added are shown in Figure 4. The color represented for buffer layer as same as the fuel type hazard-index map layer. Purple color represents the null level, blue color represents the low level, green color represents the moderate level, yellow color represents the high level, and red color represents the extreme level.

Result of the integration of four layer of hazard-index map are shown in Figure 5. All the value of FHRI of fuel type, road buffer, resident area buffer, and canal buffer was calculated to generate the final hazard-index map. The final result FHRI shows that overall of the resident area and oil palm plantation area is moderate but some area is high and extreme danger. The extreme and high spot area should be given more attention because fire hazard in this area is crucial. This matter is caused by, the residential area involved more than 10,000 lives which is covered schools, 2188 unit of houses in Taman Indera Sempurna 1 and 2, and more than 100 unit of shop buildings [60].

The road area also needs to give more attention while faced moderate and high level of FHRI. Jalan Kuantan – Pekan on the study area is the main road for pekan citizens to access Kuantan city or north region and vice versa. Year 2014 is the most worst forest fire tragedy near road on study area, lots of vehicle are crashed or accidents due to the fire hazard with the thick smoke [61].

Table 3 show the summary of the results as presented in Figure 5. Over 50% of study area faced low fire hazard, moderate fire hazard is the second highest covering 41.16% of the study area. High and extreme fire hazard area cover up to 5% in total. Even though the percentage of high and extreme fire hazard rating index seem mild, but should not be taken lightly.

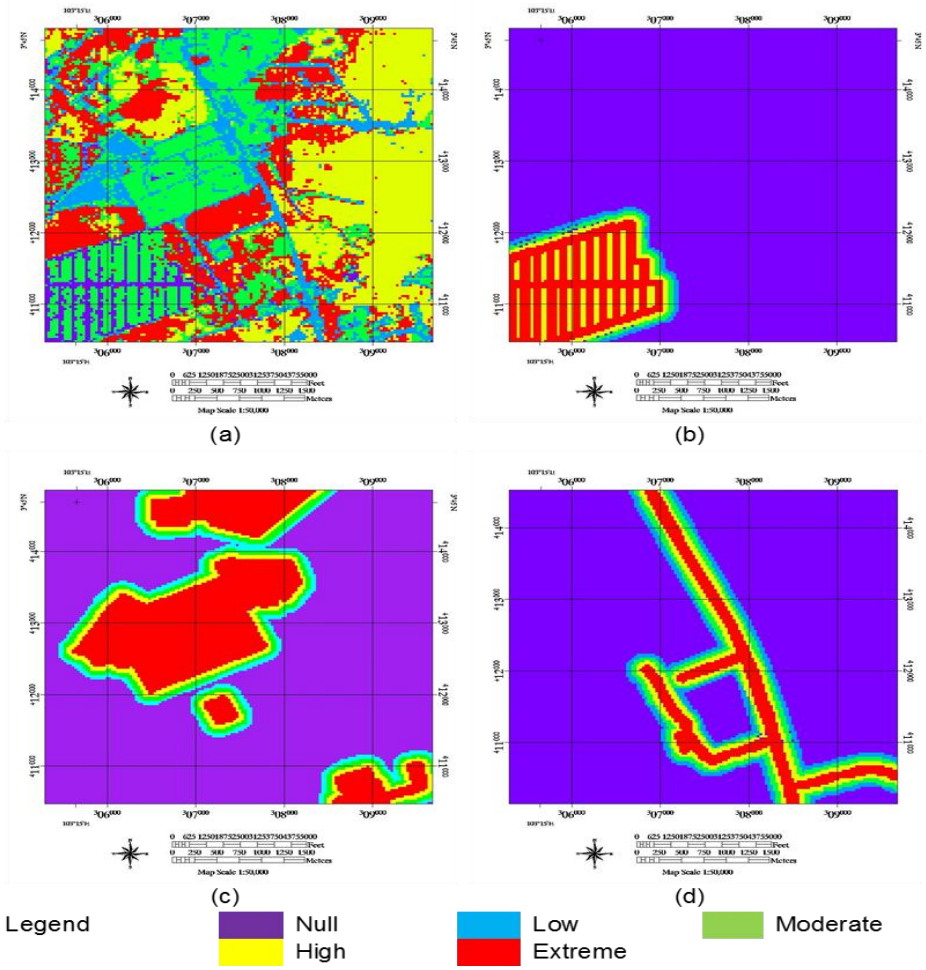

Figure 4. Fire Hazard Rating Index (FHRI) for (a) Fuel Type; (b) Canal buffer; (c) Resident Area buffer; (d) Road buffer

Ascertain the map in Figure 5, the extreme fire hazard index located near to residential and high fire hazard index is on the road. Although the fire hazard is quite related to fuel type but fire hazard rating index include both fuel type and dynamic of fire behaviour. Result shows the extreme fire hazard index not only cause by flammable fuel type such as peat land but also considered the danger tendency from constantly human access area.

Therefore, this study important not only to decide the proportion of fuel type that can easily to burn but also mapping the potential high hazard if forest fire occurred. The model as shown in table 3 considered more reliable by providing the valuable information about the most highly area will be affected by the fire hazard.

CONCLUSION

The integrated analysis of spatial variables is worthful for forest fire hazard study. Remote sensing by utilizing Landsat 8 image generate fuel type data with high accuracy using maximum likelihood classification. The fuel type for the study are widely recognized as crucial in forest fire hazard prevention and suppression due to flammable material. While GIS topographic map processing facilitate the possible in the making of buffer zone map to assist the gap of human access to the prediction of fire locator. Integration of the information from Landsat 8 image and topographic map proposed the forest fire hazard map model was performed properly in identify the potential areas subjected to a higher fire hazard. Further research should be devoted to testing the other layer of Landsat 8 such as thermal layer to predict the location of forest fire will occur. The integration of fire hazard map data with forest fire forecast will improve the study are fire hazard defence.

ACKNOWLEDGMENT

This research was supported by Grant RDU130399, RDU140335 and RDU151309 awarded to Universiti Malaysia Pahang by Ministry of Higher Education Malaysia.

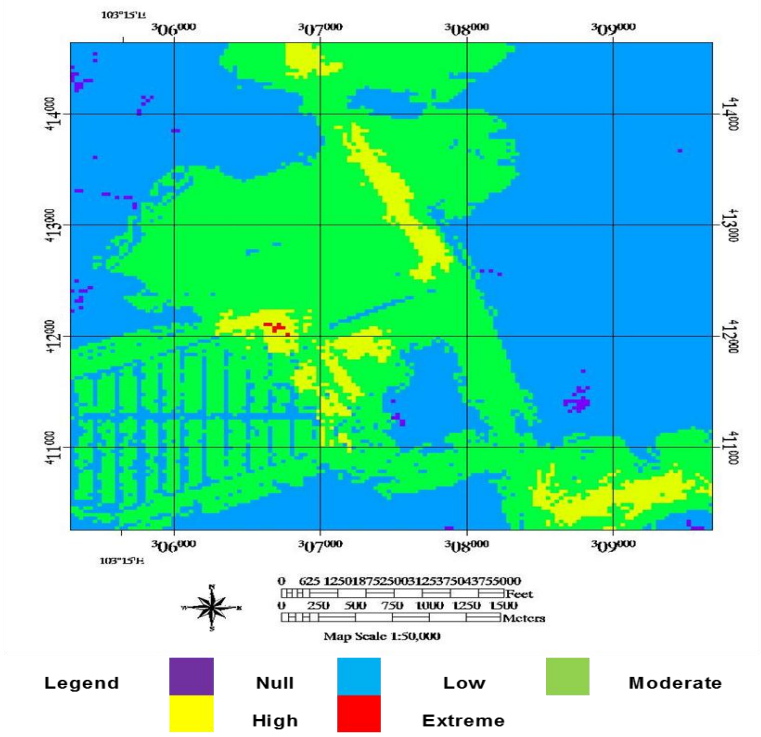

Figure 5. Hazard index map.

Table 3. Proportion of fire hazard values affected by the fire in the study area

Color Overlay	Fire Hazard Rating Index	Cover Area (%)
	Null	0.38
	Low	53.46
	Moderate	41.16
	High	4.96
	Extreme	0.04

REFERENCES

[1] J. Kucera and Y. Yasuoka, "Regional monitoring of forest disturbances and their potential effects to carbon cycling," in *Paper presented at the 22nd Asian Conference on Remote Sensing*, 2001, p. 9.

[2] L. Telesca, G. Amatulli, R. Lasaponara, M. Lovallo, and A. Santulli, "Time-scaling properties in forest-fire sequences observed in Gargano area (southern Italy)," *Ecological Modelling,* vol. 185, pp. 531-544, 2005.

[3] D. R. Weise and C. S. Wright, "Wildland fire emissions, carbon and climate: Characterizing wildland fuels," *Forest Ecology and Management,* vol. 317, pp. 26-40, 2014.

[4] P. Garcia-Chevesich, R. Valdes-Pineda, D. Neary, and R. Pizarro, "Using rainwater harvesting techniques for firefighting in forest plantations," 2015.

[5] M. Francos, X. Úbeda, J. Tort, J. M. Panareda, and A. Cerdà, "The role of forest fire severity on vegetation recovery after 18years. Implications for forest management of Quercus suber L. in Iberian Peninsula," *Global and Planetary Change,* vol. 145, pp. 11-16, 2016.

[6] M. Marlier, R. DeFries, A. Voulgarakis, P. Kinney, J. Randerson, D. Shindell*, et al.*, "El Nino and health risks from landscape fire emissions in southeast Asia, Nature Climate Change, 3, 131–136," ed, 2013.

[7] E. Martínez Ruiz, R. Vélez, C. Tot, F. Hernández, D. Saavedra, A. Wolffsohn*, et al.*, "Fire management: global assessment 2006," FAO, Roma (Italia). 9251056668, 2007.

[8] B. Gabbert. (2016, 1 Dec. 2016). *Why have fires gotten larger in recent decades?* Available: http://wildfiretoday.com/2016/10/29/why-have-fires-gotten-larger-in-recent-decades/

[9] B. Gabbert. (2016, 1 Dec. 2016). *Study concludes climate change has doubled acres burned in western U.S.* Available: http://wildfiretoday.com/2016/10/11/study-concludes-climate-change-has-doubled-acres-burned-in-western-u-s/

[10] M. Ahmad-Zainal, "Forest fire in Malaysia: Its management and impact on biodiversity," *Asean. Biodiv,* vol. 1, pp. 31-35, 2001.

[11] Bernama. (2016, 1 Dec 2016). Malaysia: 2,940 forest, bush fire outbreaks recorded in 10 days. *(Carbon & Climate)*. Available: http://www.eco-business.com/news/malaysia-2940-forest-bush-fire-outbreaks-recorded-in-10-days/

[12] Bernama, "Kebakaran Hutan Gambut Di Pahang Hampir Berjaya Dipadam," in *Bernama*, ed. Kuantan, 2007.

[13] A. PahangKu, "KEMALANGAN JALAN KUANTAN - PEKAN AKIBAT JEREBU " in *Pahangku Media* vol. 2016, A. PahangKu, Ed., ed. Kuantan, 2014.

[14] Bernama. (2016, Over 70 hectares of peatlands on fire in Pahang. Available: http://www.malaysiakini.com/news/337112

[15] Bernama, "Kebakaran Hutan Di Pahang Bertambah Luas," in *BERNAMA*, ed. Kuantan: BERNAMA, 2010.

[16] E. Chuvieco and R. G. Congalton, "Application of remote sensing and geographic information systems to forest fire hazard mapping," *Remote sensing of Environment,* vol. 29, pp. 147-159, 1989.

[17] P. Roy, "Forest fire and degradation assessment using satellite remote sensing and geographic information system," *Satellite Remote sensing and GIS applications in agricultural meteorology,* p. 361, 2003.

[18] A. Langner, J. Miettinen, and F. Siegert, "Land cover change 2002–2005 in Borneo and the role of fire derived from MODIS imagery," *Global Change Biology,* vol. 13, pp. 2329-2340, 2007.

[19] W. Liu, S. Wang, Y. Zhou, L. Wang, and S. Zhang, "Analysis of forest potential fire environment based on GIS and RS," in *Geoinformatics, 2010 18th International Conference on*, 2010, pp. 1-6.

[20] P. Biswajeet and A. Hamid, "Forest fire detection and monitoring using high temporal MODIS and NOAA AVHRR satellite images in Peninsular Malaysia," *Disaster Advances,* vol. 3, pp. 18-23, 2010.

[21] J. E. Vogelmann, J. R. Kost, B. Tolk, S. Howard, K. Short, X. Chen*, et al.*, "Monitoring landscape change for LANDFIRE using multi-temporal satellite imagery and ancillary data," *Selected Topics in Applied Earth Observations and Remote Sensing, IEEE Journal of,* vol. 4, pp. 252-264, 2011.

[22] H. Adab, K. D. Kanniah, and K. Solaimani, "Modeling forest fire risk in the northeast of Iran using remote sensing and GIS techniques," *Natural hazards,* vol. 65, pp. 1723-1743, 2013.

[23] S. N. Williamson, D. S. Hik, J. A. Gamon, J. L. Kavanaugh, and G. E. Flowers, "Estimating temperature fields from MODIS land surface temperature and air temperature observations in a sub-Arctic Alpine environment," *Remote Sensing,* vol. 6, pp. 946-963, 2014.

[24] A. Ishtiaque, S. W. Myint, and C. Wang, "Examining the ecosystem health and sustainability of the world's largest mangrove forest using multi-temporal MODIS products," *Science of the Total Environment,* vol. 569, pp. 1241-1254, 2016.

[25] M. J. Falkowski, P. E. Gessler, P. Morgan, A. T. Hudak, and A. M. Smith, "Characterizing and mapping forest fire fuels using ASTER imagery and gradient modeling," *Forest Ecology and Management,* vol. 217, pp. 129-146, 2005.

[26] N. Im, K. Kawamura, E. Suwandana, and Y. Sakuno, "Monitoring Land Use and Land Cover Effects on Water Quality in Cheung Ek Lake using ASTER Images," *American Journal of Environmental Sciences,* vol. 11, p. 1, 2015.

[27] P. Roy, A. Guha, and K. V. Kumar, "An approach of surface coal fire detection from ASTER and Landsat-8 thermal data: Jharia coal field, India," *International Journal of Applied Earth Observation and Geoinformation,* vol. 39, pp. 120-127, 2015.

[28] C. Donlon, B. Berruti, A. Buongiorno, M.-H. Ferreira, P. Féménias, J. Frerick*, et al.*, "The global monitoring for environment and security (GMES) sentinel-3 mission," *Remote Sensing of Environment,* vol. 120, pp. 37-57, 2012.

[29] M. Drusch, U. Del Bello, S. Carlier, O. Colin, V. Fernandez, F. Gascon*, et al.*, "Sentinel-2: ESA's optical high-resolution mission for GMES operational services," *Remote Sensing of Environment,* vol. 120, pp. 25-36, 2012.

[30] R. Torres, P. Snoeij, D. Geudtner, D. Bibby, M. Davidson, E. Attema*, et al.*, "GMES Sentinel-1 mission," *Remote Sensing of Environment,* vol. 120, pp. 9-24, 2012.

[31] Z. Malenovský, H. Rott, J. Cihlar, M. E. Schaepman, G. García-Santos, R. Fernandes*, et al.*, "Sentinels for science: Potential of Sentinel-1,-2, and-3 missions for scientific observations of ocean, cryosphere, and land," *Remote Sensing of Environment,* vol. 120, pp. 91-101, 2012.

[32] J. R. Jensen, "Introductory digital image processing: a remote sensing perspective," Univ. of South Carolina, Columbus1986.

[33] Y. Ke, J. Im, J. Lee, H. Gong, and Y. Ryu, "Characteristics of Landsat 8 OLI-derived NDVI by comparison with multiple satellite sensors and in-situ observations," *Remote Sensing of Environment,* vol. 164, pp. 298-313, 2015.

[34] I. D. M. R. S. N. A. M. F. Y. R. DAUD, "Kebakaran hutan kian buruk -- * Lebih 8,000 hektar musnah * Bomba hadapi kesukaran padamkan api," in *Utusan*, ed. Kuala Lumpur, 2005.

[35] R. A. Karim, "Cuaca panas cetuskan kebakaran," in *Utusan*, ed, 2002.

[36] R. MAI, "PENJARA PENOR MARKAS OPERASI PADAMKAN KEBAKARAN," in *Bernama*, ed. Kuantan, 1998.

[37] H. Metro, "Kebakaran di hutan tanah gambut di Jalan Kuantan Pekan ", ed, 2014.

[38] T. M. ROS, "KEBAKARAN KAWASAN HUTAN GAMBUT PENOR MASIH BERTERUSAN," in *Bernama*, ed. Kuantan, 2007.

[39] A. Ainuddin Nuruddin, H. M. Leng, and F. Basaruddin, "Peat moisture and water level relationship in a tropical peat swamp forest," *Journal of Applied Sciences,* vol. 6, pp. 2517-2519, 2006.

[40] R. Aniza and M. Nor, "Impact assessment of land use and land cover (LULC) changes on land surface temperature (LST) in Kuantan, Pahang," 2016.

[41] J. A. Barsi, J. L. Barker, and J. R. Schott, "An atmospheric correction parameter calculator for a single thermal band earth-sensing instrument," in *Geoscience and Remote Sensing Symposium, 2003. IGARSS'03. Proceedings. 2003 IEEE International*, 2003, pp. 3014-3016.

[42] L. Cailian, C. Jie, and L. Tongchao, "Atmospheric correction on Landsat ETM+ satellite image based on FLAASH model," *Protection Forest Science and Technology,* vol. 5, pp. 46-48, 2008.

[43] O. Rudjord and O. Trier, "Evaluation of FLAASH atmospheric correction," *Norwegian Computer Centre. Norwegian. 24p,* 2012.

[44] F. Pacifici, "An automatic atmospheric compensation algorithm for very high spatial resolution imagery and its comparison to FLAASH and QUAC," *Proc. JACIE,* pp. 1-43, 2013.

[45] D. Helder, L. Leigh, N. Mishra, S. Mackin, and C. T. Pinto, "Vicarious Calibration–Let the Data Do All the Work!," 2015.

[46] G. Chander, B. L. Markham, and D. L. Helder, "Summary of current radiometric calibration coefficients for Landsat MSS, TM, ETM+, and EO-1 ALI sensors," *Remote sensing of environment,* vol. 113, pp. 893-903, 2009.

[47] R. Bhatt, D. R. Doelling, D. Morstad, B. R. Scarino, and A. Gopalan, "Desert-based absolute calibration of successive geostationary visible sensors using a daily exoatmospheric radiance model," *IEEE Transactions on Geoscience and Remote Sensing,* vol. 52, pp. 3670-3682, 2014.

[48] J. Richards and X. Jia, "Remote sensing digital image analysis Springer," *Berlin, Germany,* 1999.

[49] H. Jeffreys, "An invariant form for the prior probability in estimation problems," in *Proceedings of the Royal Society of London a: mathematical, physical and engineering sciences*, 1946, pp. 453-461.

[50] R. A. Schowengerdt, *Techniques for image processing and classifications in remote sensing*: Academic Press, 2012.

[51] P. Mather and B. Tso, *Classification methods for remotely sensed data*: CRC press, 2016.

[52] A. Asmala, "Analysis of maximum likelihood classification on multispectral data," *Applied Mathematical Sciences,* vol. 6, pp. 6425-6436, 2012.

[53] J. Sun, J. Yang, C. Zhang, W. Yun, and J. Qu, "Automatic remotely sensed image classification in a grid environment based on the maximum likelihood method," *Mathematical and Computer Modelling,* vol. 58, pp. 573-581, 2013.

[54] A. Ahmad and S. Quegan, "Analysis of maximum likelihood classification technique on Landsat 5 TM satellite data of tropical land covers," in *Control System,*

Computing and Engineering (ICCSCE), 2012 IEEE International Conference on, 2012, pp. 280-285.

[55] M. Slim, J. T. Perron, S. J. Martel, and K. Singha, "Topographic stress and rock fracture: a two- dimensional numerical model for arbitrary topography and preliminary comparison with borehole observations," *Earth Surface Processes and Landforms,* vol. 40, pp. 512-529, 2015.

[56] A. Usup, Y. Hashimoto, H. Takahashi, and H. HAYASAKA, "Combustion and thermal characteristics of peat fire in tropical peatland in Central Kalimantan, Indonesia," *Tropics,* vol. 14, pp. 1-19, 2004.

[57] M. Hasmadi, H. Pakhriazad, and M. Shahrin, "Evaluating supervised and unsupervised techniques for land cover mapping using remote sensing data," *Geografia-Malaysian Journal of Society and Space,* vol. 5, 2017.

[58] A. Asmala and Q. Shaun, "The Effects of Haze on the Accuracy of Maximum Likelihood Classification," *Applied Mathematical Sciences,* vol. 10, pp. 1935-1944, 2016.

[59] L. J. Jansen, M. Bagnoli, and M. Focacci, "Analysis of land-cover/use change dynamics in Manica Province in Mozambique in a period of transition (1990–2004)," *Forest Ecology and Management,* vol. 254, pp. 308-326, 2008.

[60] D. Portal. (2017). *Demographic Statistics Third Quarter (Q3) 2017, Malaysia*. Available: https://www.dosm.gov.my/v1/index.php?r=column/cthemeByCat&cat=430&bul_id=MFpnNGw4RnZmRnNKeC80Q25DZUgzZz09&menu_id=L0pheU43NWJwRWVSZklWdzQ4TlhUUT09

[61] BERNAMA, "Asap kebakaran hutan di jalan Kuantan-Pekan ganggu lalu lintas," in *Kosmo*, ed. Kuantan, 2014.